Original Paper

Eletrônica de Potência
Open Journal of Power Electronics



Received September 16, 2026; Received in revised form October 05, 2026; Accepted October 16, 2026; Date of publication November 11, 2026.
The review of this paper was arranged by Associate Editor Renata O. de Sousa and Editor-in-Chief Allan F. Cupertino.
*Digital Object Identifier http://doi.org/10.18618/REP.e202640*

# Operator-Oriented Blackstart Restoration Planning for Active Distribution Networks via QSTS-Based Multi-Objective Co-Simulation

**Lucas F. S. Azeredo**[1,2,*], **Jussara F. Fardin**[2], **Helder R. de O. Rocha**[2]

[1]Federal Institute of Espírito Santo (IFES), Linhares, ES, Brazil.
[2]Federal University of Espírito Santo (UFES), Graduate Program in Electrical Engineering, Vitória, ES, Brazil.

e-mail: lucas.azeredo@ifes.edu.br*; jussara.fardin@ufes.br; helder.rocha@ufes.br.
*Corresponding author.

**ABSTRACT** Blackstart restoration in active distribution networks requires switching strategies capable of balancing restoration speed, voltage recovery quality, and operational feasibility under heterogeneous distributed energy resources and unbalanced conditions. This paper presents an operator-oriented multi-objective framework for blackstart restoration planning based on MATLAB–OpenDSS quasi-static time-series (QSTS) co-simulation. Candidate plans are assessed through chronological simulations with time-indexed voltage constraints, while a feasibility-preserving repair mechanism enforces logical energization dependencies among inverter-based and dispatchable sources, reactive support devices, and load blocks. The problem jointly minimizes the integral of time-weighted absolute error (ITAE) of voltage deviations and the total restoration time, and a genetic algorithm generates Pareto-optimal plans revealing the trade-off between faster service recovery and smoother voltage stabilization. The framework is evaluated on the IEEE 123-bus feeder, in which the staged re-energization is referenced to a firm voltage source rather than to an autonomously formed island. Representative non-dominated solutions are analyzed through switching schedules and per-phase voltage trajectories at critical buses: the ITAE is reduced by 56% at the cost of a 36% increase in restoration time, and all trajectories remain within the admissible band. The framework thus provides operationally meaningful restoration alternatives for decision support under different priorities.

**KEYWORDS** Blackstart, distribution system restoration, multi-objective optimization, quasi-static time series (QSTS), MATLAB–OpenDSS co-simulation, ITAE

## I. INTRODUCTION

The restoration of large-scale power outages requires carefully designed strategies for the staged re-energization of the network [1], [2]. In active distribution networks, this task is substantially more challenging due to the increasing penetration of distributed generation (DG), inverter-based resources, reactive support devices, and inherently unbalanced operating conditions [3]. Restoration actions must be executed under strict voltage limits while accounting for sequential switching effects, source coordination, and the risk of voltage excursions that may trigger protection systems or stress sensitive equipment [4]. Blackstart is the process of re-energizing a de-energized network from resources able to start without an external supply, progressively rebuilding the system until normal supply is resumed. At the distribution level this is therefore no longer a purely procedural task, but a constrained decision-making problem involving multiple interacting resources and conflicting operational objectives.

Conventional practice still relies heavily on operator experience and predefined rule-based procedures, which become increasingly limited as distribution systems evolve toward higher operational complexity, particularly under renewable intermittency, converter-dominated resources, and heterogeneous controllable assets [5], [6]. To address combinatorial and nonlinear power-system decision problems, evolutionary metaheuristics have been widely adopted in optimal power flow, distributed generation placement, and network reconfiguration [7], and more recent studies explore hybrid and large-scale multi-objective approaches for constrained mixed-integer planning with renewable resources, battery energy storage, and intertemporal constraints [8]. Blackstart and service restoration studies have likewise incorporated renewable variability, multi-objective criteria, and operational constraints [4], [9]. Nevertheless, distribution-level formulations that explicitly combine *(i)* chronological restoration assessment, *(ii)* feasibility-preserving switching logic, and *(iii)* operator-oriented analysis of the trade-off between restoration speed and voltage recovery quality remain limited. In particular, few studies evaluate restoration plans in unbalanced feeders through time-indexed simulations that


CC BY

reflect staged switching and the operational dependencies among dispatchable sources, reactive support devices, and load blocks.

From an operational perspective, restoration quality cannot be characterized solely by service pickup speed, since delayed or poorly damped voltage deviations along the restoration trajectory may compromise equipment performance and practical feasibility. The integral of time-weighted absolute error (ITAE) is adopted here as a dynamic performance index because it penalizes persistent deviations and favors faster settling behavior, a criterion that remains relevant both in classical control and in recent power-system optimization studies concerned with dynamic response quality [10], [11]. The conference version of this work [12] minimized the energy not supplied (ENS) together with the recovery time; being an aggregate energy measure, the ENS is insensitive to *how* the voltage evolves between switching stages, and the ITAE is adopted here as the complementary criterion that resolves this trajectory-quality dimension.

Motivated by these gaps, this paper proposes an operator-oriented multi-objective framework for distribution-level blackstart restoration in active and unbalanced feeders, integrating a genetic-algorithm-based search with a MATLAB–OpenDSS QSTS co-simulation procedure and a feasibility-preserving mechanism for energization dependencies among diesel generators, photovoltaic (PV) units, capacitor banks, reactors, and load blocks. Rather than seeking a single optimal sequence, the approach generates non-dominated restoration plans that expose the trade-off between restoration speed and voltage recovery quality. The framework is assessed on the IEEE 123-bus unbalanced feeder [13], [14] within a MATLAB–OpenDSS environment [15], showing how representative Pareto-optimal solutions lead to distinct switching timelines and voltage recovery profiles at critical buses.

## II. RELATED WORK AND CONTRIBUTIONS

Representative studies on restoration and multi-objective planning in active distribution networks leave distinct gaps with respect to the problem addressed here. Reviews of blackstart with renewable and distributed resources map the control and planning requirements of the problem but remain at the survey level and are largely oriented to the transmission system [4]. Response-based and coordination-based restoration formulations determine which loads to pick up and from which sources, yet they evaluate the restored configuration rather than the chronological path taken to reach it, so that the quality of the voltage recovery between switching stages is not an explicit criterion [9], [16]. Large-scale multi-objective evolutionary approaches have been applied to distributed-resource planning with storage and intertemporal constraints, but on a planning horizon rather than on a switching sequence [8]. Finally, the conference version of this work optimized the energy not supplied jointly with the recovery time [12], an aggregate measure insensitive to how the voltage evolves between stages.

Against this background, the main contributions of this work are:

1) an operator-oriented multi-objective formulation jointly accounting for restoration speed and voltage recovery quality through an ITAE-based metric in unbalanced feeders;
2) a feasibility-preserving sequencing strategy that enforces energization dependencies among distributed sources, reactive support devices, and load blocks, preventing operationally inconsistent plans during the search;
3) a chronological MATLAB–OpenDSS QSTS co-simulation framework for evaluating restoration trajectories under staged switching and time-indexed voltage constraints;
4) a decision-support interpretation of Pareto-optimal plans, linking optimization outcomes to switching schedules and per-phase voltage behavior at critical buses.

## III. PROBLEM FORMULATION

Let $\mathbf{x} \in \{0,1\}^{451}$ denote a binary decision vector that authorizes the participation of controllable elements (DG, PV, capacitor banks, reactors, and load blocks). Two objectives are minimized simultaneously: an ITAE-based voltage recovery metric and the plan restoration time. Fig. 1 summarizes the framework; the implementation of each block is detailed in Section V.

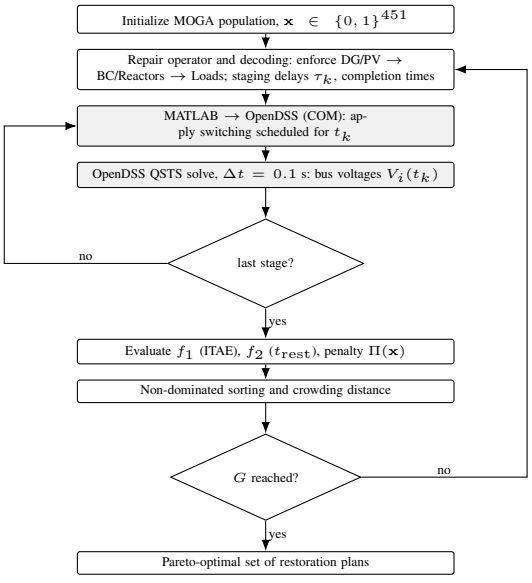



**FIGURE 1. MATLAB–OpenDSS co-simulation and optimization loop. Shaded blocks are executed by OpenDSS.**

### A. Objective Functions

Voltage trajectories are evaluated at a representative set of critical buses $\mathcal{B}_{\text{crit}} = \{40, 47, 60, 76, 83, 92, 103, 112\}$ and on the available phases $\Phi_i$ at each bus $i$. The aggregated voltage error is

$$\bar{e}(t;\mathbf{x}) = \frac{1}{|\mathcal{B}_{\text{crit}}|} \sum_{i\in\mathcal{B}_{\text{crit}}} \frac{1}{|\Phi_i|} \sum_{\phi\in\Phi_i} |V_{\text{ref}} - V_{i,\phi}(t;\mathbf{x})|\,, \quad (1)$$

where $V_{\text{ref}} = 1.0$ p.u. and $V_{i,\phi}(t;\mathbf{x})$ is the per-phase voltage magnitude. The first objective is the ITAE of the aggregated error,

$$f_1(\mathbf{x}) = \sum_{t=0}^{T} t\ \bar{e}(t;\mathbf{x}), \quad (2)$$

which penalizes late deviations more heavily and promotes faster stabilization [10]. The second objective is the restoration time,

$$f_2(\mathbf{x}) = t_{\text{rest}}(\mathbf{x}), \quad (3)$$

defined as the completion time of the last energized element in the plan, as detailed in Section V, Subsection C.

### B. Constraints and Penalties

At each simulation step, OpenDSS computes the bus voltages of the updated network, and operational feasibility is enforced through the admissible voltage band:

$$V_i^{\min} \le V_i(t;\mathbf{x}) \le V_i^{\max}, \qquad \forall i, t. \quad (4)$$

Violations of the voltage band, unsatisfied dependencies, or dependency cycles are penalized through a nonnegative term $\Pi(\mathbf{x})$ added to both objectives during ranking:

$$F_1(\mathbf{x}) = f_1(\mathbf{x}) + \lambda\,\Pi(\mathbf{x}), \qquad F_2(\mathbf{x}) = f_2(\mathbf{x}) + \mu\,\Pi(\mathbf{x}), \quad (5)$$

with $\lambda, \mu \gg 0$, so that no infeasible plan survives into the non-dominated set. The numerical values adopted for the limits, staging delays, and resource ratings are consolidated in Table 2.

### C. Multi-Objective Genetic Algorithm (MOGA)

A multi-objective genetic algorithm (MOGA) is employed to explore non-dominated restoration strategies by simultaneously minimizing conflicting objectives [7]. Each candidate is encoded as a binary vector representing the energization state of controllable elements (DGs, PV units, capacitor banks, reactors, and load blocks), and logical dependencies are enforced by a repair operator that preserves the hierarchy DG/PV → Capacitors/Reactors → Loads. Its configuration is listed in Table 1, and its application to the restoration problem is explained in Section V, Subsection D.

**TABLE 1. MOGA configuration parameters**

| Parameter | Value |
|---|---|
| Population size ($N$) | 100 |
| Chromosome length ($L$) | 451 |
| Number of generations ($G$) | 100 |
| Crossover probability ($p_c$) | 0.7 |
| Mutation probability ($p_m$) | 0.01 |
| Selection method | Tournament |
| Crossover type | Single-point |
| Mutation type | Bit-flip |
| Elitism | Enabled |

## IV. QUASI-STATIC TIME-SERIES SIMULATION

QSTS simulation analyzes the system through a sequence of steady-state solutions at discrete time steps. Each step is a quasi-stationary operating point: fast switching transients are not resolved, and network variables are approximated by their phasor values for the prevailing conditions of loads, distributed energy resources (DERs), and switching states. This contrasts with electromagnetic transient (EMT) simulation, where high-frequency phenomena require much smaller integration steps and detailed device switching models [17]. The approach follows the QSTS methodology widely used in distribution-system studies [18], [19], and is appropriate when the relevant operational changes occur over seconds to minutes, while fast electromagnetic transients are not critical to the study objectives.

Let $t_k$ denote the discrete instants of a QSTS simulation with constant step $\Delta t$:

$$t_k = t_0 + k\Delta t, \qquad k = 0, 1, \ldots, K. \quad (6)$$

At each instant $t_k$ the scheduled switching actions are applied, the steady-state model is solved for the updated topology and injections, the voltage constraints are checked, the time-aggregated indices are updated, and the simulation advances to $t_{k+1}$. The evolution is stepwise and event-driven, so the stage-to-stage voltage excursions—rather than waveform-level transients—are quantified consistently across candidate sequences. This suits optimization loops, where many switching policies are evaluated under identical conditions without the burden of EMT simulation for every candidate.

The scope of the approximation must be stated explicitly: QSTS does not resolve sub-cycle dynamics and therefore cannot reproduce inrush currents, power-electronic switching behavior, or fast converter interactions immediately after energization. When such effects materially influence the decision, an EMT–QSTS co-simulation is appropriate, escalating fidelity only for the most promising candidates [17], [20]. For the questions addressed here—voltage-band compliance after each switching action and time-aggregated performance along the horizon—the quasi-static representation is sufficient.

## V. METHODOLOGY

The proposed framework couples MATLAB (orchestration and optimization) with OpenDSS (power-flow and time-domain simulation), enabling the evaluation of restoration sequences in unbalanced feeders by integrating the logical activation of devices with their electrical response. For every candidate vector generated by the MOGA, MATLAB issues


CC BY

sequential commands to OpenDSS via its COM interface. OpenDSS is operated in time mode with time-based control, so that each solution advances the simulation clock by a fixed step of $\Delta t = 0.1$ s and each energization stage is followed by the staging delay of the corresponding device class. The recorded voltages are used to evaluate the objective functions, and constraint violations trigger penalty terms that reduce the dominance rank of infeasible solutions. The division of tasks between the two tools is shown in Fig. 1.

### A. Test Feeder

The IEEE 123-bus feeder is a detailed benchmark for testing optimization and control methods in distribution systems [13]. It models a medium-voltage network at 4.16 kV with mixed overhead/underground sections, multi-phase laterals, and unbalanced loading [14], while voltage regulators and shunt capacitor banks provide voltage support and introduce interacting control layers during switching operations [16]. The OpenDSS implementation is adopted here for its support of time-series simulation and MATLAB-based co-simulation [15]. The topology, line data, and unbalanced load allocation are those of the published benchmark [13], [14] and are not reproduced here.

### B. Resource Models and Converter Representation

The restoration is referenced to a stiff voltage source (`Vsource`, bus 1, 4.16 kV, 1.00 p.u., three-phase short-circuit level of 2000 MVA) that provides the voltage and angle reference required by the phasor solution throughout the restoration horizon. The substation source of the benchmark model is disabled at the start of every simulation, so this reference is the only external anchor of the system, and the trajectories reported here characterize the staged re-energization of the feeder *against a firm voltage reference* rather than the autonomous formation of an unreferenced island. Unlike the experimentally assessed grid-forming schemes of [21], [22], the present formulation does not reproduce that control layer. The four diesel units are dispatched against this reference as voltage-controlled sources, modeled in OpenDSS as `Generator` objects (4.16 kV, 100 kVA, Model 3, $V_{pu} = 1.0$) connected at buses 150, 47, 60, and 83, and provide the local voltage support that precedes PV enabling and load pickup. The 91 PV plants are grid-following, inverter-interfaced resources modeled as `PVSystem` objects; they can only be enabled after the dispatchable units are synchronized and supporting the local voltage, which is the physical reason for the ordering enforced by the repair operator. Reactive support is represented in aggregated form: a lumped three-phase capacitor bank at bus 150, whose rating is selected in ten weighted steps spanning 0–3900 kvar, and a lumped three-phase reactor at the same bus with fixed impedance ($R = 0.01\ \Omega$, $X = 0.1\ \Omega$). The phasor formulation also implies that frequency is not a state of the model: the diesel units are represented by their steady-state voltage-control behavior, without governor droop, inertial response, or load-damping dynamics, and no frequency constraint enters the optimization. Frequency excursions during load pickup are therefore not captured, and the staging delays of Table 2 act as the only proxy for the time a unit needs to stabilize before the next block is connected. Because the QSTS formulation represents converters through their steady-state power injections, the inverter dynamics are captured only through their capability limits, and the apparent-power rating acts as the binding constraint at each restoration stage. The load data follow the IEEE 123-bus benchmark specification [13], and the remaining simulation parameters are consolidated in Table 2.

**TABLE 2. Simulation, constraint, and resource parameters**

| Parameter | Value | Resource | Value |
|---|---|---|---|
| $\Delta t$ | 0.1 s | Voltage ref. (bus 1) | `Vsource`, 1.00 p.u. |
| Horizon $T$ | plan-dependent | | 2000 MVA |
| $V^{\min}/V^{\max}$ | 0.95 / 1.05 p.u. | Diesel (4 units) | 100 kVA, 4.16 kV |
| $T_{\text{hold}}$ | 30 s | | Model 3 |
| *Staging delays* ($\tau_k$) | | PV plants | 91 `PVSystem` |
| Diesel sync. | 60 s | Capacitor (bus 150) | 0–3900 kvar, 10 steps |
| PV enabling | 20 s | Reactor (bus 150) | $R = 0.01$, $X = 0.1\ \Omega$ |
| Cap./reactor sw. | 5 s | Load blocks | 91, IEEE 123 benchmark |
| Load-block pickup | 10 s | | |
| Fixed idle | 0.1 s | | |

### C. Decision-Vector Encoding (451 Binary Variables)

Each candidate restoration plan is encoded by a binary vector $\mathbf{x} \in \{0,1\}^{451}$ that specifies *what* to energize and implicitly *when* each device completes its energization, given logical dependencies and the staging delays realized in simulation. The index ranges of $\mathbf{x}$ are organized as shown in Table 3.

**TABLE 3. Mapping of the 451 binary decision variables**

| Block | Description | Indices in $\mathbf{x}$ |
|---|---|---|
| BC sizing | weighted kvar steps | 1–10 |
| BC participation | activation flags | 11–128 |
| Reactor sizing | impedance selection bits | 129–136 |
| PV units | on/off flags for PV plants | 137–227 |
| Reactor participation | activation flags | 228–356 |
| Diesel generators | on/off flags (4 units) | 357–360 |
| Load blocks | on/off flags for loads | 361–451 |

A value $x_k = 1$ authorizes device $k$ to participate in the plan, but the *completion* time of each device depends on both the satisfaction of upstream dependencies and the staging delay of its class. Dependencies are encoded via a binary matrix $D \in \{0,1\}^{451\times 451}$, where $D_{k\ell} = 1$ means device $k$ requires device $\ell$ to be active beforehand.[1] With $P_k := \{\ell \mid D_{k\ell} = 1,\ x_\ell = 1\}$, the completion time of device $k$ follows

$$t_k = \begin{cases} \tau_k, & x_k = 1,\ P_k = \varnothing, \\ \max\limits_{\ell \in P_k} t_\ell + \tau_k, & x_k = 1,\ P_k \neq \varnothing, \\ -\infty, & x_k = 0, \end{cases} \tag{7}$$

[1] In practice: Diesel → PV/BC; BC → Reactors; Reactors → Loads.

where $\tau_k$ is the staging delay of the device class, listed in Table 2. The plan restoration time is $t_{\text{rest}} = \max_{k:\, x_k=1} t_k$, and cycles or unsatisfied dependencies incur a large penalty (infeasible plan).

The sizing bits of the capacitor block jointly select the rating of the lumped bank, while the participation bits of the capacitor and reactor blocks authorize their insertion in the sequence; for PVs, diesels, and load blocks, the bits act as on/off authorizations. In the reported results the reactive support is aggregated at a single bus with the reactor impedance held fixed, so the reactor sizing bits do not alter the electrical model; they are retained in the encoding for compatibility with the distributed-placement formulation left for future work. This encoding assumes that every controllable element has an independently operable switching device, which is an idealization: in present distribution networks remote switching is typically available at feeder and lateral level rather than per load block, so the decision space explored here is an upper bound on the flexibility an operator would actually command. Communication latency and breaker actuation times are not modeled separately; they are absorbed into the staging delays $\tau_k$ of Table 2, which set the minimum interval between consecutive actions of each device class. Coarser, more realistic switching granularity would reduce the dimension of $\mathbf{x}$ and the attainable resolution of the Pareto front, but it does not change the structure of the formulation. Evaluation proceeds in a fixed priority pass (Diesel $\rightarrow$ PV/BC $\rightarrow$ Reactors $\rightarrow$ Loads), but the actual completion times are governed by (7); hence two plans with the same active set can yield different $t_{\text{rest}}$ depending on dependency chaining and on the selected capacitor rating.

### D. Monitored Buses and Optimization Process

The set $\mathcal{B}_{\text{crit}}$ used in (1) was selected to cover upstream, mid-feeder, and downstream locations and to expose the worst-case voltage excursions during staged restoration. Buses 47, 60, and 83 lie at the diesel connection points, where local voltage control is strongest; buses 40 and 76 are mid-feeder nodes influenced by several switching stages, serving as sentinels for excursion propagation; buses 92 and 112 are lateral/remote nodes where voltage is more sensitive to topology and reactive support; and bus 103 is the far-end node of the critical-load area, useful to verify steady-state compliance after full pickup. In addition to $\mathcal{B}_{\text{crit}}$, buses 9, 25, and 65 are monitored for verification of lateral behavior and are reported in Fig. 3, but they do not enter the ITAE aggregation of (1).

The MOGA introduced in Section III, Subsection C, is applied as follows. Each generation begins with the initialization or reproduction of individuals, followed by simulation and evaluation of their objective functions; solutions are then ranked through non-dominated sorting and refined with a crowding-distance measure to ensure proper spread along the Pareto front [7]. The repair operator embedded in the decoding process guarantees that each energization sequence adheres to the hierarchy DG/PV $\rightarrow$ Capacitors/Reactors $\rightarrow$ Loads. Beyond preventing invalid switching combinations, this hierarchy reproduces an operator-inspired restoration procedure: the dispatchable units must be synchronized first to support the voltage at their connection points, after which inverter-based PV units and reactive support are coordinated before progressive load pickup. Enforcing this ordering therefore guarantees physical executability and avoids evaluating switching permutations that would not be considered in practice.

## VI. RESULTS AND DISCUSSION

### A. Pareto Front Analysis

Fig. 2 presents the Pareto front obtained for the proposed blackstart restoration problem, in which the ITAE is evaluated against the total restoration time ($t_{\text{rest}}$). The front is well distributed and exhibits a clear monotonic trade-off: faster restoration plans tend to be associated with larger cumulative voltage deviations, whereas smoother voltage recovery is achieved at the expense of longer restoration times. This confirms that restoration speed alone is insufficient to characterize restoration quality in active distribution networks, since the chronological electrical behavior during staged energization also plays a relevant operational role.

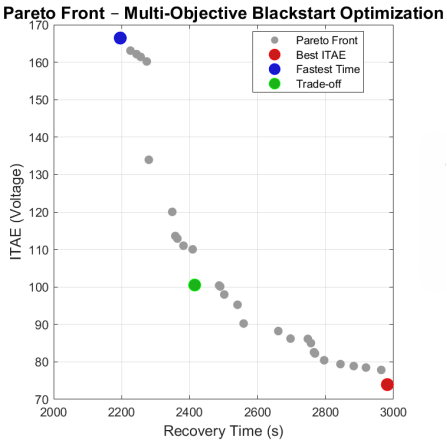



**FIGURE 2. Pareto front of the multi-objective blackstart optimization (ITAE vs. recovery time). Highlighted points: Fastest Time (blue), Trade-off (green), and Best ITAE (red).**

Three representative non-dominated solutions were selected for detailed discussion—*Fastest Time*, *Trade-off (knee point)*, and *Best ITAE*—whose objective values are given in Table 4. Moving from the *Fastest Time* to the *Best ITAE* plan reduces the ITAE by 56% while increasing the restoration time by 36%; the knee point captures 71% of the total ITAE reduction for only 28% of the additional time. The *Fastest Time* plan energizes larger portions of the system earlier and picks up load with reduced temporal separation between switching actions: the final restored state remains feasible, but the voltage security margin during the early and intermediate stages is narrower, which makes such plans


CC BY

inherently less conservative. The *Trade-off* solution adopts a more gradual schedule that allows the coordinated insertion of reactive support and distributed sources before the pickup of heavier load blocks. The *Best ITAE* solution uses longer effective intervals before connecting additional load blocks, producing the most homogeneous electrical response at the price of a longer restoration time; it is therefore relevant when voltage quality and equipment stress reduction are prioritized over the fastest possible service recovery.

**TABLE 4. Objective values of the representative Pareto-optimal solutions**

| Solution | ITAE | $t_{\text{rest}}$ (s) |
|---|---|---|
| Fastest Time | 166.5 | 2195 |
| Trade-off (knee) | 100.5 | 2415 |
| Best ITAE | 74.0 | 2975 |

Overall, the conflict between restoration time and voltage recovery quality is structurally relevant rather than marginal. The intermediate region of the front indicates that moderate increases in restoration time can produce substantial gains in voltage performance, whereas moving toward the extreme minimum-ITAE region yields progressively smaller improvements relative to the additional delay, reinforcing the practical relevance of the knee-point solution.

### *B. Voltage Trajectories and Switching Chronology*

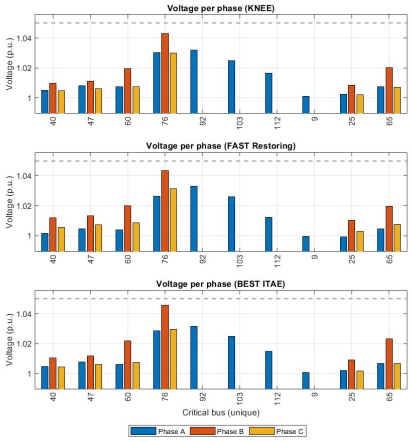



**FIGURE 3. Per-phase voltages at the critical buses for the three Pareto-optimal cases: *KNEE*, *FAST Restoring*, and *BEST ITAE*.**

Figs. 4 and 5 describe the time evolution of voltages at the critical buses during staged energization, while Fig. 3 emphasizes the final per-phase operating points after restoration completion, enabling a joint assessment of voltage security along the trajectory and of phase behavior at the final condition. Two observations must be separated. First, in all three plans the voltages remain inside the admissible 0.95–1.05 p.u. band throughout the entire restoration horizon, with all recorded values contained within 0.975–1.005 p.u.; no candidate among the analyzed solutions violates the operating limits at any stage. Second, the trajectories nevertheless

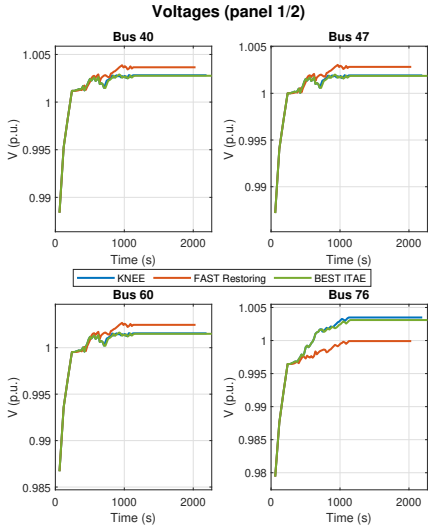



**FIGURE 4. Voltages (panel 1/2): per-phase voltages under QSTS for the *FAST Restoring*, *KNEE*, and *BEST ITAE* solutions.**

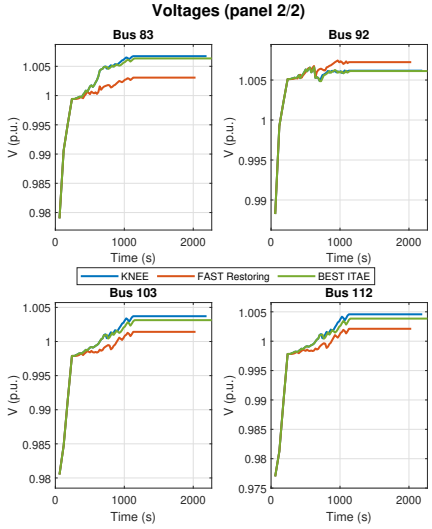



**FIGURE 5. Voltages (panel 2/2): per-phase voltages under QSTS for the same three solutions, showing the steady-state clustering around the nominal range and the phase imbalance among them.**

differ systematically, and the ordering of these differences follows the ITAE ranking.

The *FAST Restoring* case exhibits the sharpest stage-to-stage changes and the widest spread of per-phase values, reflecting the aggressive pickup pattern and a correspondingly smaller margin with respect to the admissible limits during intermediate stages. The *KNEE* solution shows a more coordinated progression, with reduced phase dispersion and smoother transitions, consistent with the knee-point interpretation observed in the Pareto front. The *BEST ITAE* case presents the smoothest and most homogeneous behavior, with the lowest voltage stress during staged restoration

and final per-phase values more tightly grouped around the nominal region. These differences, although systematic and consistent along the front, are small in absolute terms—within 0.01 p.u. among the three plans—so the benefit of the ITAE-oriented plans lies in the additional security margin retained during the intermediate stages, not in avoiding limit violations.

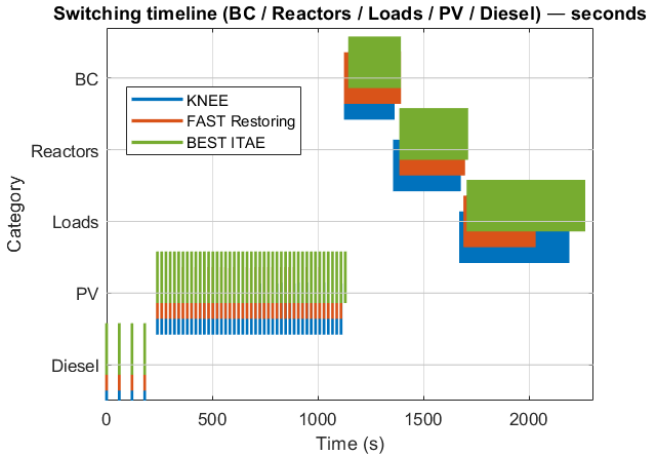



**FIGURE 6. Switching timeline for the three Pareto-optimal strategies, showing the energization sequence of Diesel → PV → BC → Reactors → Loads.**

The relationship between switching actions and voltage behavior becomes clearer in Fig. 6. The energization sequence shows that the observed voltage evolution is not a numerical artifact of the optimization process, but a direct consequence of the adopted restoration logic: the prior insertion of voltage-forming sources and reactive support prepares the feeder for subsequent reactor connection and load pickup, improving voltage regulation along the horizon and explaining the smoother responses of the more conservative solutions.

Feasibility is assessed by the joint satisfaction of two conditions: completion of the switching schedule, which defines $t_{\mathrm{rest}}$, and a per-bus restored condition requiring $V_i(t)$ to stay inside the admissible band for at least $T_{\mathrm{hold}}$; plans failing either are penalized. The voltage trajectories should therefore be read as chronological restoration paths rather than final operating snapshots.

### *C. Limitations*

Six limitations delimit the scope of the reported results. First, the reported front corresponds to a single execution of the MOGA, with no statistical campaign or quality indicators, so it is a representative outcome of the adopted configuration rather than a converged estimate of the true front. Second, no alternative algorithm was used as a benchmark, so the performance of the adopted MOGA against comparators such as NSGA-II or SPEA2 remains open. Third, reactive support is aggregated at a single bus, so its spatial allocation is not optimized. Fourth, the assessment is restricted to a single benchmark feeder; validation on a real Brazilian distribution network, for which public data are available, would strengthen the external validity of the conclusions and is left for future work. Fifth, the restoration is assessed against the firm voltage reference of Section V, Subsection B, so the trajectories do not characterize the stability of a fully autonomous island, where the dynamic response of the grid-forming units would govern the post-switching behavior [23]. Sixth, as detailed in Section IV, sub-cycle phenomena are outside the modeling scope. None of them affects the internal consistency of the comparison, since all candidates are evaluated under identical settings, but they bound the generality of the reported values.

## VII. CONCLUSION

This paper presented an operator-oriented multi-objective framework for blackstart restoration in active distribution systems, jointly minimizing the ITAE of voltage deviations and the total restoration time while representing the sequential energization dependencies among distributed generators, reactive support devices, and load blocks inside a MATLAB–OpenDSS QSTS co-simulation loop.

For the unbalanced IEEE 123-bus feeder, the ITAE was reduced by 56% between the fastest and the smoothest plans at the cost of a 36% longer restoration, with the knee point retaining 71% of that gain for only 28% of the additional time. All plans kept the critical-bus voltages inside the 0.95–1.05 p.u. band throughout the horizon, so the differences among them concern the security margin preserved during the intermediate stages rather than compliance at the final operating point. The framework therefore delivers Pareto-optimal alternatives for decision-making under different operational priorities instead of a single optimal solution. Future work will address the limitations of Section VI, Subsection C: a statistical campaign with quality indicators, benchmarking against established multi-objective algorithms, distributed placement and sizing of reactive support, and reintroduction of the ENS criterion of [12] jointly with the ITAE.

## ACKNOWLEDGMENT

The authors thank FAPES, CNPq, and the Federal Institute of Espírito Santo for supporting this work; the corresponding grants are listed under Funding.

## NOTE TO READERS

This article extends the paper presented at the 18th Brazilian Power Electronics Conference (COBEP 2025) [12], adding the quasi-static time-series formalization (Section IV), the aggregated multi-bus ITAE formulation that replaces the energy-based criterion of [12], the operator-oriented reading of the Pareto front, and an expanded voltage-trajectory analysis.


CC BY

## AUTHOR'S CONTRIBUTIONS

**L.F.S.AZEREDO:** Conceptualization, Formal Analysis, Methodology, Software, Validation, Visualization, Writing – Original Draft. **J.F.FARDIN:** Conceptualization, Project Administration, Supervision, Writing – Review & Editing. **H.R.O.ROCHA:** Methodology, Resources, Supervision, Writing – Review & Editing.

## PLAGIARISM POLICY

This article was submitted to the similarity system provided by Crossref and powered by iThenticate – Similarity Check.

## DATA AVAILABILITY

The data used in this research is available in the body of the document.

## REFERENCES


[1] M. M. Adibi, *Power System Restoration: Methodologies and Implementation Strategies*, IEEE Press, Piscataway, NJ, USA, 2000, URL: https://www.wiley-vch.de/en/areas-interest/engineering/energy-10eg/power-technology-power-engineering-10eg4/power-system-restoration-978-0-7803-5397-8.

[2] North American Electric Reliability Corporation (NERC), *Standard EOP-005-3: System Restoration from Blackstart Resources*, North American Electric Reliability Corporation, 2014, URL: https://www.nerc.com/pa/Stand/Reliability%20Standards/EOP-005-3.pdf.

[3] P. Kundur, *Power System Stability and Control*, McGraw-Hill, New York, NY, USA, 1994.

[4] Z. Pan, N. Jenkins, J. Wu, "Black start from renewable energy resources: Review and a case study of Great Britain", *Renewable and Sustainable Energy Reviews*, vol. 209, p. 115143, 2025, doi:10.1016/j.rser.2024.115143.

[5] M. Panteli, P. Mancarella, "The grid: Stronger, bigger, smarter? Presenting a conceptual framework of power system resilience", *IEEE Power and Energy Magazine*, vol. 13, no. 3, pp. 58–66, 2015, doi:10.1109/MPE.2015.2397334.

[6] H. A. Oliveira, L. H. S. Santos, L. A. d. S. Ribeiro, J. G. de Matos, L. d. P. A. Pinheiro, "Challenges in Microgrids with Medium Voltage Circuit", *Eletrônica de Potência*, vol. 30, p. e202511, 2025, doi:10.18618/REP.e202511.

[7] K. Deb, A. Pratap, S. Agarwal, T. Meyarivan, "A fast and elitist multiobjective genetic algorithm: NSGA-II", *IEEE Transactions on Evolutionary Computation*, vol. 6, no. 2, pp. 182–197, 2002, doi:10.1109/4235.996017.

[8] A. Ali, A.-u.-R. Bughio, G. Abbas, M. U. Keerio, N. H. Mugheri, S. Memon, A. S. Saand, "Optimization of distributed energy resources planning and battery energy storage management via large-scale multi-objective evolutionary algorithm", *Energy*, vol. 311, p. 133463, 2024, doi:10.1016/j.energy.2024.133463.

[9] Y. Wang, Y. Xu, J. He, C.-C. Liu, K. P. Schneider, M. Hong, D. T. Ton, "Coordinating Multiple Sources for Service Restoration to Enhance Resilience of Distribution Systems", *IEEE Transactions on Smart Grid*, vol. 10, no. 5, pp. 5781–5793, 2019, doi:10.1109/TSG.2019.2891515.

[10] D. Graham, R. C. Lathrop, "The synthesis of optimum transient response: Criteria and standard forms", *Transactions of the American Institute of Electrical Engineers, Part II: Applications and Industry*, vol. 72, no. 5, pp. 273–288, 1953, doi:10.1109/TAI.1953.6371346.

[11] S. Habib, G. Abbas, T. A. Jumani, A. A. Bhutto, S. Mirsaeidi, E. M. Ahmed, "Improved Whale Optimization Algorithm for Transient Response, Robustness, and Stability Enhancement of an Automatic Voltage Regulator System", *Energies*, vol. 15, no. 14, p. 5037, 2022, doi:10.3390/en15145037.

[12] L. F. S. Azeredo, J. F. Fardin, H. R. O. Rocha, "Multiobjective Optimization of Blackstart in Distribution Systems Using Genetic Algorithm Considering ENS and System Recovery Time", *in 2025 18th Brazilian Power Electronics Conference (COBEP)*, 2025.

[13] W. H. Kersting, "Radial distribution test feeders", *in IEEE Power Engineering Society Winter Meeting*, pp. 908–912, New York, NY, USA, 1991, doi:10.1109/PESW.2001.916993.

[14] W. H. Kersting, *Distribution System Modeling and Analysis*, 4th ed., CRC Press, 2018, doi:10.1201/9781315120782.

[15] R. C. Dugan, D. Montenegro, *The Open Distribution System Simulator (OpenDSS): Reference Guide*, Electric Power Research Institute (EPRI), Washington, DC, USA, 2018, URL: https://sourceforge.net/p/electricdss/code/HEAD/tree/trunk/Distrib/Doc/OpenDSSManual.pdf.

[16] A. Gholami, F. Aminifar, "A Hierarchical Response-Based Approach to the Load Restoration Problem", *IEEE Transactions on Smart Grid*, vol. 8, no. 4, pp. 1700–1709, 2017, doi:10.1109/TSG.2015.2503320.

[17] F. Escudié, F. Caignet, N. Nolhier, M. Bafleur, "From Quasi-Static to Transient System Level ESD Simulation: Extraction of Turn-On Elements", *in 2016 38th Electrical Overstress/Electrostatic Discharge Symposium (EOS/ESD)*, pp. 1–10, Garden Grove, CA, USA, 2016, doi:10.1109/EOSESD.2016.7592563.

[18] D. Montenegro, R. C. Dugan, M. J. Reno, "Open Source Tools for High Performance Quasi-Static-Time-Series Simulation Using Parallel Processing", *in 2017 IEEE 44th Photovoltaic Specialists Conference (PVSC)*, 2017, doi:10.1109/PVSC.2017.8521538.

[19] J. A. Azzolini, M. J. Reno, N. S. Gurule, K. A. W. Horowitz, "Evaluating Distributed PV Curtailment Using Quasi-Static Time-Series Simulations", *IEEE Open Access Journal of Power and Energy*, vol. 8, pp. 365–376, 2021, doi:10.1109/OAJPE.2021.3111821.

[20] D. Y. Raval, S. N. Pandya, "Electromagnetic Transient (EMT) and Quasi-Static Time Series (QSTS) Co-Simulation for Analyzing Integration of Power-Electronics-Based Generation/Power Quality Improvement Solution in Secondary Distribution Networks", *Electric Power Systems Research*, vol. 253, p. 112572, 2026, doi:10.1016/j.epsr.2025.112572.

[21] G. V. Ramos, T. M. Parreiras, B. J. Cardoso Filho, "Control Performance Assessment of a Zero Harmonic Distortion Grid-Forming Converter for Medium Voltage Islanded Microgrids", *Eletrônica de Potência*, vol. 29, p. e202441, 2024, doi:10.18618/REP.e202441.

[22] J. M. T. do Amaral, J. S. Ramos, C. C. M. de Souza, G. J. da Silva, E. L. van Emmerik, R. F. S. Dias, "Grid-Forming Fuel Cell System for an Islanded AC Grid", *Eletrônica de Potência*, vol. 29, p. e202457, 2024, doi:10.18618/REP.e202457.

[23] A. W. dos S. Serra, L. A. d. S. Ribeiro, M. Savaghebi, "Disturbance Decoupling in Grid-Forming Inverters for Enhanced Dynamic Response", *Eletrônica de Potência*, vol. 30, p. e202528, 2025, doi:10.18618/REP.e202528.


## BIOGRAPHIES

**Lucas F. S. Azeredo** received the B.Sc. and M.Sc. degrees in Electrical Engineering from UFES, Vitória, Brazil, where he is pursuing the Ph.D. degree. He is a Professor at IFES, Linhares Campus, working on power system restoration and multi-objective optimization.

**Jussara F. Fardin** received the B.Sc. degree from UFES in 1978, the M.Sc. from PUC-Rio in 1983, and the Ph.D. from UNICAMP in 2001, all in Electrical Engineering. She is a Full Professor at UFES, working on energy management, microgrids, and smart grids.

**Helder R. de O. Rocha** received the B.Sc. degree in Electrical Engineering and the M.Sc. and Ph.D. degrees in Scientific Computing and Power Systems from UFF, Brazil. He is an Associate Professor at UFES and a CNPq Fellow (PQ-2), working on artificial intelligence, metaheuristics, and smart grids.